NASA CONTRACTOR REPORT

NASA CR-1501

TESTS ON PROPELLERS UNDER STATIC THRUST CONDITIONS

by J. Brusse, A. E. Cronk, and C. F. Kettleborough

Prepared by
TEXAS A&M UNIVERSITY
College Station, Texas
for Langley Research Center

NATIONAL AERONAUTICS AND SPACE ADMINISTRATION • WASHINGTON, D. C. • DECEMBER 1969

TESTS ON PROPELLERS UNDER STATIC THRUST CONDITIONS

By J. Brusse, A. E. Cronk, and C. F. Kettleborough

Prepared under Grant No. NGR-44-001-011 by
TEXAS A&M UNIVERSITY
College Station, Texas

for Langley Research Center

NATIONAL AERONAUTICS AND SPACE ADMINISTRATION

For sale by the Clearinghouse for Federal Scientific and Technical Information
Springfield, Virginia 22151 – Price $3.00

TESTS ON PROPELLERS UNDER STATIC THRUST CONDITIONS

By J. Brusse, A. E. Cronk, and C. F. Kettleborough

SUMMARY

This report describes the experimental equipment which has been built at Texas A&M University to measure the performance of a propeller-torque, thrust and flow fields. The test data shows that for an activity factor of 100, blade plan-form at tip speeds ranging from 400 to 900 fps is not a strong parameter in determining gross performance.

INTRODUCTION

The problem of accurately predicting the aerodynamic loading on a propeller or rotor blade is one of the most important problems facing the designer of helicopters or propeller driven aircraft. Since 1944 the rapid increase in helicopter, STOL (short take-off and landing), VTOL (vertical take-off and landing) technology has brought with it the realization that many of the basic approximations inherent in the classical propeller theories must be reexamined in the light that the vertical velocity that generates lift is large compared to the flight velocity. Much detailed work has been carried out on helicopter rotors. In Reference 1, static thrust measurements were made; in Reference 2, induced velocities in the wake were measured. However, propellers have not received the same degree of attention. Some results have been reported in References 3 and 4 in which thrust, and torque were measured and flow patterns were obtained.

In order to test propeller blade configurations under static thrust conditions a dynamometer has been designed and constructed with the propeller rotating in a horizontal plane. Instrumentation has been added to measure thrust and torque utilizing strain gage bridges. Air flow mapping equipment enables the three components of velocity to be measured in both the inflow and wake regions of the propeller.

A series of propellers have been tested. The first two were used primarily during the development of the dynamometer and the data acquisition instrumentation and in running repeatability tests designed to provide assessment of the reliability of the data. A further set of three propellers incorporated only plan-form variations while the other physical parameters were maintained constant.

After gathering data at all the desired combinations of blade angle and rotational speeds, the data are reduced to coefficient form for plotting and subsequent evaluation.

SYMBOLS

b	Blade width
h	Maximum blade thickness
C_L	Lift coefficient
C_P	Power coefficient $P/\rho N^3 D^5$
C_T	Thrust coefficient $T/\rho N^2 D^4$
D	Propeller diameter (ft)
FM	Figure of Merit
N	Rotational speed (r.p.s.)
P	Power
r, z	Cylindrical coordinate system. The z direction is positive downwards (See Figure 2)
r_p	Radius of propeller tip
$\bar{r}$	Normalized radius $r = \bar{r}\, r_p$
u, v, w	Velocities in r, θ, z directions respectively.
$\bar{u}, \bar{v}, \bar{w}$	Velocities normalized with respect to Ωr_p
V_t	Velocity of tip of propeller
z , $\bar{z}$	Coordinate perpendicular to propeller plane $z = \bar{z}\, r_p$
Ω	Angular velocity
ρ	Density
ϕ , θ	Velocity component directions defined in Figure 2.

EXPERIMENTAL EQUIPMENT AND TECHNIQUES

Description of Dynamometer

The propeller static thrust dynamometer designed to minimize wake and inflow interference was constructed in a large airplane hangar at the Texas A&M Research Annex. The configuration of the dynamometer provides for rotation of the test propeller in a horizontal plane with the line of thrust acting vertically upward. Rotation is accomplished by a shaft which turns inside a 7.5 inch diameter, vertically mounted tubular steel housing. The housing has four slanted legs welded to its lower end which are bolted to reinforced concrete piers extending eleven feet deep into the earth (Figure 1).

Two 275 hp V-8 marine engines are installed to drive the vertical shaft through a differential gear box. The differential gearing is required for drawing power from both engines without having to achieve precise speed synchronization of the engines. Engine cooling is accomplished with tap water that is admitted to each engine through water pressure regulators. The heated water is expelled outside the hangar through the exhaust pipes and is not recirculated through the engines. Fuel is piped to both engines from a 500 gallon skid tank which is located outside and about fifty feet from the hangar. Both water and fuel pipes have electric solenoid valves that are operated by the engine ignition switches. Couplings which allow for installation misalignment and vibration isolation are installed between each engine output shaft and the gear box shafts. An overrunning clutch is mounted between the differential gear box output shaft and the main drive shaft to prevent sudden shaft stoppage and possible damage to the propeller balance in case of mechanical failure in either of the power trains or gear box. The engine hydraulic clutches, carburetor controls and differential gear box brakes are operated by remotely controlled electric actuators through suitable linkages. Controls for starting, clutch engagement, and engine speed regulation along with instruments for monitoring engine cooling, oil pressure, electrical system battery charging and engine rpm are mounted on a panel in a concrete control house.

The rotational speed of a test propeller is measured by an electric tachometer that operates from pulses generated by a magnetic pick-up placed close to a 60-tooth steel gear which rotates with the propeller drive shaft.

Thrust and torque measurements are made with a two-component strain gage balanced mounted between a flange at the end of the propeller shaft and the propeller hub. Both the thrust and torque components utilize strain gage bridges having four active arms with the excitation and signal voltages being transmitted through a slip-ring assembly. Cables are routed from the stationary member of the slip-ring assembly into the control house where appropriate connections are made to the bridge excitation power supplies and the signal amplifier and read-out equipment. Bridge excitation is provided by two 0-10 volt regulated power supplies and signal amplification is provided by DC low level amplifiers. A span and balance circuit is provided for both the thrust and torque components along with appropriate switches and circuitry to permit insertion of calibration resistance.

The electric tachometer circuit is connected to an electronic counter which presents the propeller rotational speed in rpm on its digital display. The thrust signal is connected to a digital voltmeter through the appropriate amplifier and balance control unit while the torque signal is connected to an integrating digital voltmeter in a similar manner.

All three instruments are connected to a digital scanner and thence to a tape printer. The scanner is a programmable device that controls the sampling and storage of data in digital form until all sources are ready for printing whereupon it gives print commands to the printer. As normally operated with the propeller dynamometer for performance testing, the scanner gates all three digital instruments simultaneously so that the sampling periods begin together. Each instrument then samples for its preset period of time and the resulting values, in digital form, are stored in the scanner. When all sampling is completed, the scanner releases the stored data to the printer which is printed in a sequence and format previously programmed into the scanner.

Static calibration of the balance and electronic data acquisition equipment is accomplished by loading the balance in both thrust and torque with weights that act through suitable levers and bell cranks. Dynamic rotating calibration of the torque component has not been done because of the complexity of equipment required but the thrust component has been calibrated both statically and with the propeller shaft rotating. The results of the two methods of calibration indicated that the signal was not affected significantly with the shaft running as compared with the signal transmitted while the shaft was stationary. Tests with the slip-ring assembly to determine brush noise indicated that the signal to noise ratio through the assembly was not objectionable.

Airflow Mapping Equipment and Technique

While performance testing is useful in evaluating specific propellers, it does not provide the kind of detailed airflow information required by the theorist. Therefore, it was considered necessary to evaluate the direction and speed of the air at selected points both in the wake of the propeller and in the inflow region ahead of the propeller.

The general airflow in the wake of a propeller operating in the static thrust condition can be characterized as a contracting helical flow for some distance downstream of the propeller disc. In order to completely describe the airflow at specified points in that kind of flow field the axial, radial and rotational components must be known. Figure 2 presents a graphic description of the axis system and sign convection used in the evaluation of the wake airflow.

An instrument transport was devised and erected at the dynamometer site to facilitate the placement of airflow sampling instrumentation in both the inflow and wake regions of the propeller. The transport consists of a vertical column placed nine feet away from and parallel to the dynamometer shaft housing, a remotely controllable trolley that travels up and down the column, and a remotely

controllable platform mounted on the trolley that moves horizontally along a radius between the drive shaft centerline and the platform. The vertical and horizontal travel of the transport provides for sampling the airflow anywhere in a radial plane having dimensions approximately 14 feet axially by 3 1/2 feet radially in the propeller wake region and about 3 feet axially by 3 1/2 feet radially in the inflow region. In addition to the remote, variable speed controls provided for both axial and radial movement of the instrument transport, a remote position indicating system was installed so that a probe can be positioned anywhere within the limits of the above mentioned radial plane to an accuracy of 1/16 inch both axially and radially. The position indicating system consists of synchromotor transmitters, geared to the transport drive mechanism, electrically connected to synchro-motor receivers that are in turn geared to high speed mechanical counters. The drive gearing to the transmitters and the gearing between the receivers and the counters is arranged to provide read-out in inches and hundredths of inches on the counters. The instrument transport is heavily constructed and built to close tolerances so that a very steady platform for instrumentation mounting is provided and any uncertainty of probe positioning results from the flexibility inherent in small probes and their mounting booms.

A two-axis, null type directional sensing probe was constructed that permits measurement of both the radial and tangential angle components of the air velocity vector representing the airflow at any point of interest within the travel limits of the instrument transport. In addition to the two-axis angular measurement capability, the probe also has a total head tube and a static pressure probe (Figure 3). The flow direction sensor is moved by reversible electric gear-motors that are remotely operated from the operating console. Angle indicating devices for both the tangential and radial angles are located in the control house along with the operating controls.

The differential pressure sensed by each pair of the directional probe tubes is connected pneumatically to differential pressure transducers, the electrical outputs of the transducers are connected through span and balance circuits to the digital voltmeters. Pressures sensed by the total head and static pressure probes are connected to separate pressure transducers with their electrical outputs also being routed through span and balance controls to the digital voltmeters. Selection of the pressure source indications to be displayed on the voltmeters is made by use of an appropriate switching arrangement.

In operation, the probe is first moved to the desired measurement position by use of the instrument transport and its associated controls. When in position the probe is rotated about one axis to bring one pair of direction sensing tubes approximately to a null position. The probe is then rotated about its other axis to bring the remaining pair of tubes approximately to a null position. The null positions (zero differential pressure across a pair of tubes) are then refined by manipulation of the appropriate controls and the radial and tangential angles assumed by the probe are read from the angle indicators in the control room. The coarse null position is detected by use of two water filled U-tube manometers and the refined or final null positions are adjusted by reference to the digital voltmeter readings which were previously adjusted to read zero for a zero differential pressure sensed by the transducer.

After the null position of the probe has been obtained the digital voltmeters are switched over to the total and static pressure transducers whereupon their electrical outputs are read. Conversion of the observed values to engineering units is accomplished by applying the appropriate system calibration factor for each probe. Since the total head tube is directed into the airstream at the point of interest by virtue of the two-axis nulling feature, the total pressure observations are subject only to probe errors and alignment errors are minimized.

The static pressure probe is mounted on the instrument support mast centerline three inches away from the tip of the directional and total head sensing probe. This arrangement requires two probe positioning operations in order to evaluate the airflow velocity vector at the desired point of measurement. If, however, the distance between successive points of measurement is planned properly, one probe setting will allow angular and total head pressure values to be made at one point while the static pressure is read at another desired measurement point thus minimizing double setting of the probe.

Upon calibrating the probe assembly in the Texas A&M University 7 foot by 10 foot low speed wind tunnel, both directional probe pairs exhibited linear curves of almost identical slope and adequate sensitivity. The total head tube when oriented into the airflow with both directional tube pairs nulled indicated total pressure within +6% of that indicated by the total pressure orifice of the wind tunnel's pitot-static probe. The static pressure probe calibration was also checked and was found to be within - 1% of the calibration factor accompanying the instrument.

In order to provide visual evaluation of the airflow surrounding the propeller, a smoke generator with appropriate nozzles has been developed. A slavestroke unit permits a gas discharge flashtube to be synchronized at any desired propeller speed. Photographs can be made. These photographs show the general inflow pattern of air into the propeller as well as the vortex system that is formed in the wake of the propeller. The helical path of the airflow in the propeller slipstream is also observable, thus the introduction of smoke at various points around the rotating propeller provides three-dimensional evaluation of the flow phenomenon associated with the propeller operating in the static thrust condition.

EXPERIMENTAL RESULTS

Several different propeller models have been tested on the static thrust dynamometer to determine their performance characteristics. The propeller geometric characteristics are described in Figures 4 through 8.

A typical test run involves setting the desired blade angle, normally at the .75 radial station, and then rotating the propeller at selected speeds while thrust, torque, and rpm values are recorded. The excursion through the rpm range is made in steps rather than continuously to allow the rpm and airflow to stabilize for a few seconds before recording the data. After completing the rpm excursion, the dynamometer is stopped, the blade angle is reset to the next desired angle and the propeller is again run through the rpm range.

After gathering data at all the desired combinations of blade angles and rotational speeds, the data are reduced to coefficient form for plotting and subsequent evaluation.

Propellers A and B were used primarily during the development of the dynamometer and the data acquisition instrumentation and in running repeatability tests designed to provide assessment of the reliability of the data generated on the dynamometer. Propeller A was designed and manufactured several years ago for use with a tilt-wing VTOL model tested in the Langley 30 ft. by 60 ft. low speed wind tunnel. Propeller B is of a model of a propeller currently in use on a tilt-wing VTOL aircraft. Figure 9 shows the results of two tests made at different times and after different balance calibrations. On the basis of the static balance calibrations and the observed repeatability of the data, it is estimated that the dynamometer consistently provides data within 2% of the thrust and torque values provided by the test propeller. While no reliable quantitative data have been gathered concerning the effects of air recirculation inside the hangar on the propeller undergoing test, it is believed that these effects are minimal and not of great significance. Because of the lack of this knowledge, however, it is not possible to state precisely the accuracy of observed performance as related to the absolute values of thrust and torque the propeller would have if operated in an infinitely large unobstructed airspace. Figure 10 gives the performance characteristics of propeller A.

The blades of propellers C, D, and E incorporate only planform variations while the other physical parameters were maintained constant. The purpose of the series of test performed with this family of propellers was to determine the contribution of blade planform on the performance characteristics of the propeller.

The following parameters were identical in the three sets of blades:

Activity Factor = 100
Diameter = 5 ft.
Integrated design $C_L = 0$
Series 63 airfoil sections
Twist distribution
Thickness distribution

Using a 3-way and a 4-way hub, preliminary tests were made of 2, 3, or 4 blade configuration. For the 2 and 3 blade configurations the combined system dynamics of the test facility and the propeller models limited the operating ranges obtainable within acceptable vibration levels. The vibration levels were monitored by an accelerometer mounted on the main drive-shaft support. It was decided to limit the test program to the 4 blade configuration.

In the test program the blade angle setting at .75 radius was varied from 7.5 degrees to 22.5 degrees. Rotational speeds ranged from 1500 to 3500 rpm providing a tip speed range of 400 to 900 feet per second.

At each blade angle setting the rotational speed was increased with measurements being made of rpm, thrust and torque at several discrete speeds. As rotational speed was decreased the same quantities were measured at intermediate speeds. Typically, thirty sets of measurements were made at each blade angle.

A total of over 500 points were recorded. No consistent hysteresis effect, indicative of recirculation effects, could be determined. For each series of runs pressure, temperature and humidity measurements were made for calculation of air density.

At blade angles above 15 degrees, thrust and torque load limitations of the balance system prevented operation at the higher rotational speeds.

The data were reduced to standard dimensionless form of C_P (power coefficient) and C_T (thrust coefficient) using the propeller convention. From these the power figure of merit was calculated.

Both C_T and C_P showed a consistent increase with tip speed at blade angles of 17.5 degrees and below. A linear variation appeared to fit the data well so a linear fairing of the data was made and values of C_T and C_P at tip speeds of 400, 600, 800, and 900 fps were read.

The gross performance of the three sets of blades are shown as plots of C_T versus C_P in Figures 11, 12, and 13. The normal taper plan-form (propeller D) exhibits slightly better performance above $C_P = .07$.

The power figure of merit variation is presented in Figures 14, 15, and 16. It should be emphasized that the blades tested were designed only to provide plan-form variation with no attempt to optimize performance. The trends in the figure of merit variations are similar for the three sets of blades. Again the normal taper plan-form shows higher values of figure of merit at power coefficients above .08.

The data from the test program are presented in Figure 17 in the form of the ratio C_T/C_P versus C_P. The data points shown are for all plan-forms at tip speeds ranging from 400 to 900 fps. A single curve appears to fit the data reasonably well. This suggests that blade plan-form is not a strong parameter in determining gross performance, at least for an activity factor of 100.

Figures 18 and 19 show typical velocity distributions for a propeller of 5 feet diameter, series 63 airfoil with $\beta_{0.75r} = 12.5°$, and normal taper plan-form (propeller D). At 2000 rpm the tip speed is 523.6 feet per second. Of particular interest is the fact that each maximum of the vr distribution is associated with a maximum in the axial velocity distribution.

CONCLUDING REMARKS

A static thrust stand and associated measuring equipment have been developed and tested. A series of tests have been carried out on propellers differing only in plan-form variations. The results showed that for a design $C_L = 0$ and for an activity factor of 100 blade plan-form had little measurable effect on performance. Some flow surveys were made. These results showed that after contracting to about 0.8x the propeller tip radius at about two radii downstream of the propeller the slipstream started to expand.

REFERENCES

1. John P. Rabbott. Static-Thrust Measurements of the Aerodynamic Loading on a Helicopter Rotor Blade. NACA TN 3688, 1956.

2. Harry H. Heyson. Measurements of the Time-Averaged and Instantaneous Induced Velocities in the Wake of a Helicopter Rotor Hovering at High Tip Speeds. NASA TN D-393, 1960.

3. Adams, G. N. Propellor Research at Canadair Limited. Proceedings CAL/AVLABS Symposium, Vol. I (1966).

4. Borst, H. V. and Ladden, R. M. Propeller Testing at Zero Velocity. Proceedings CAL/AVLABS Symposium, Vol. I (1966).

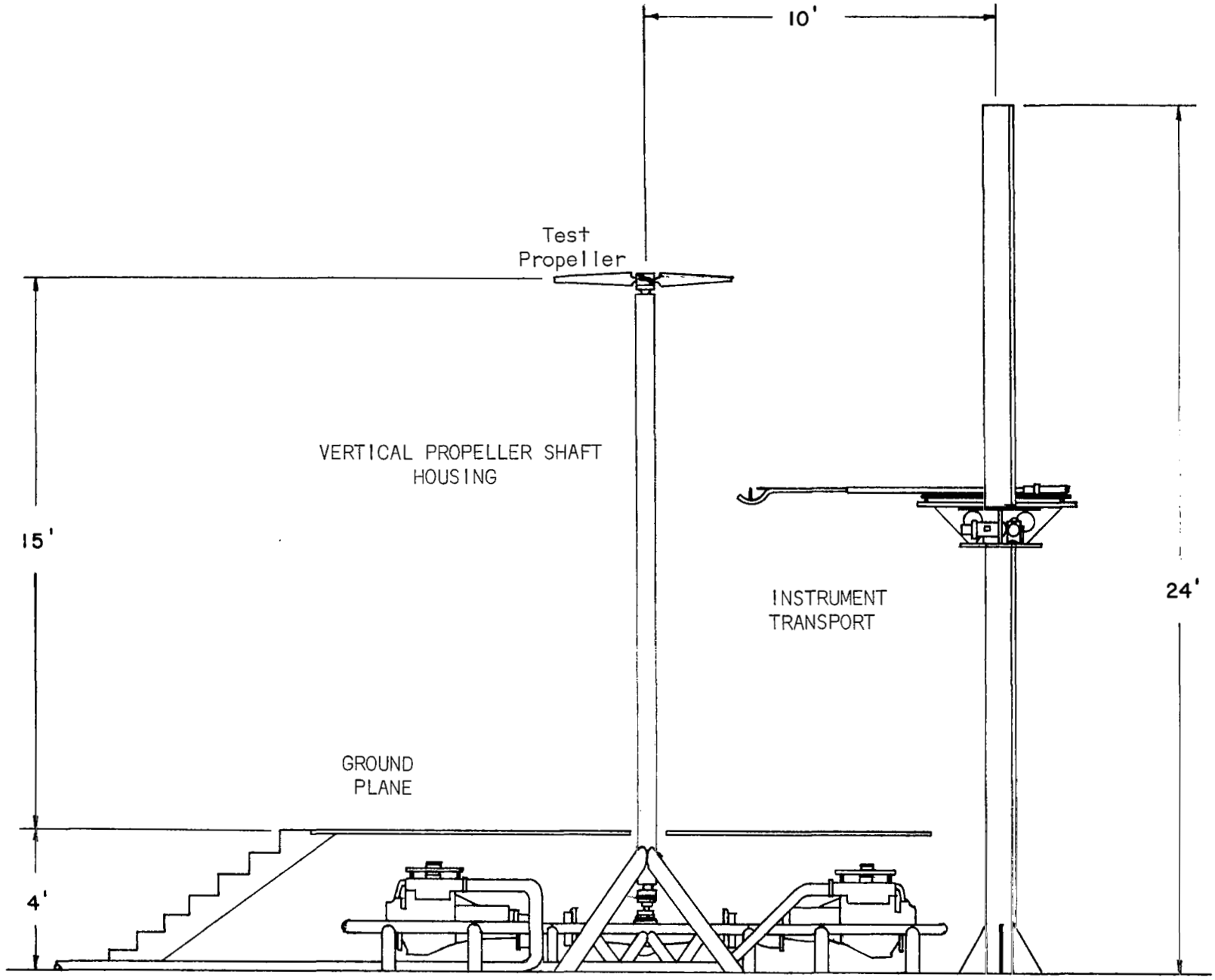

Figure 1 General Arrangement Of Test Facility

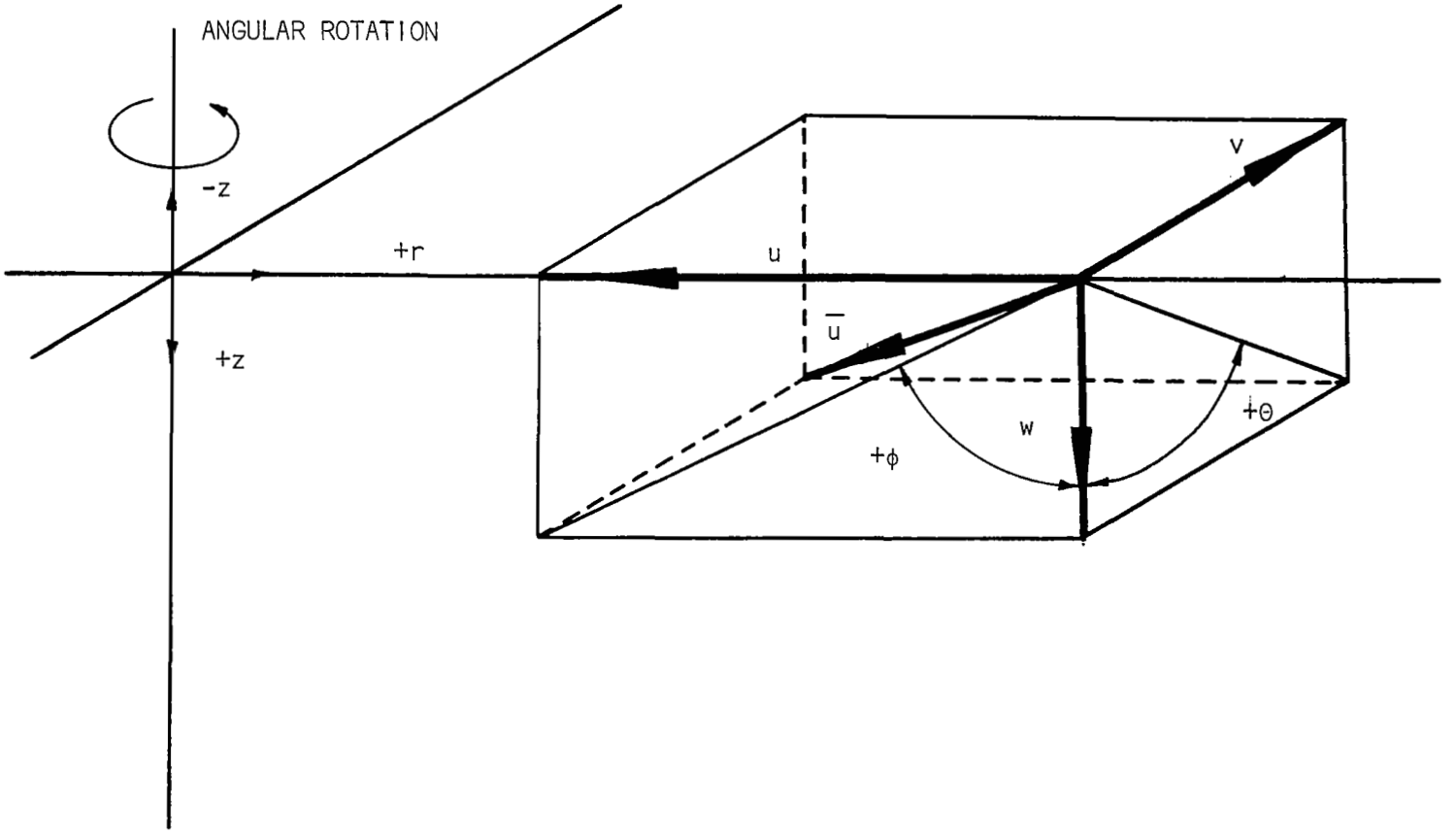

Figure 2 Velocity Components And Angles

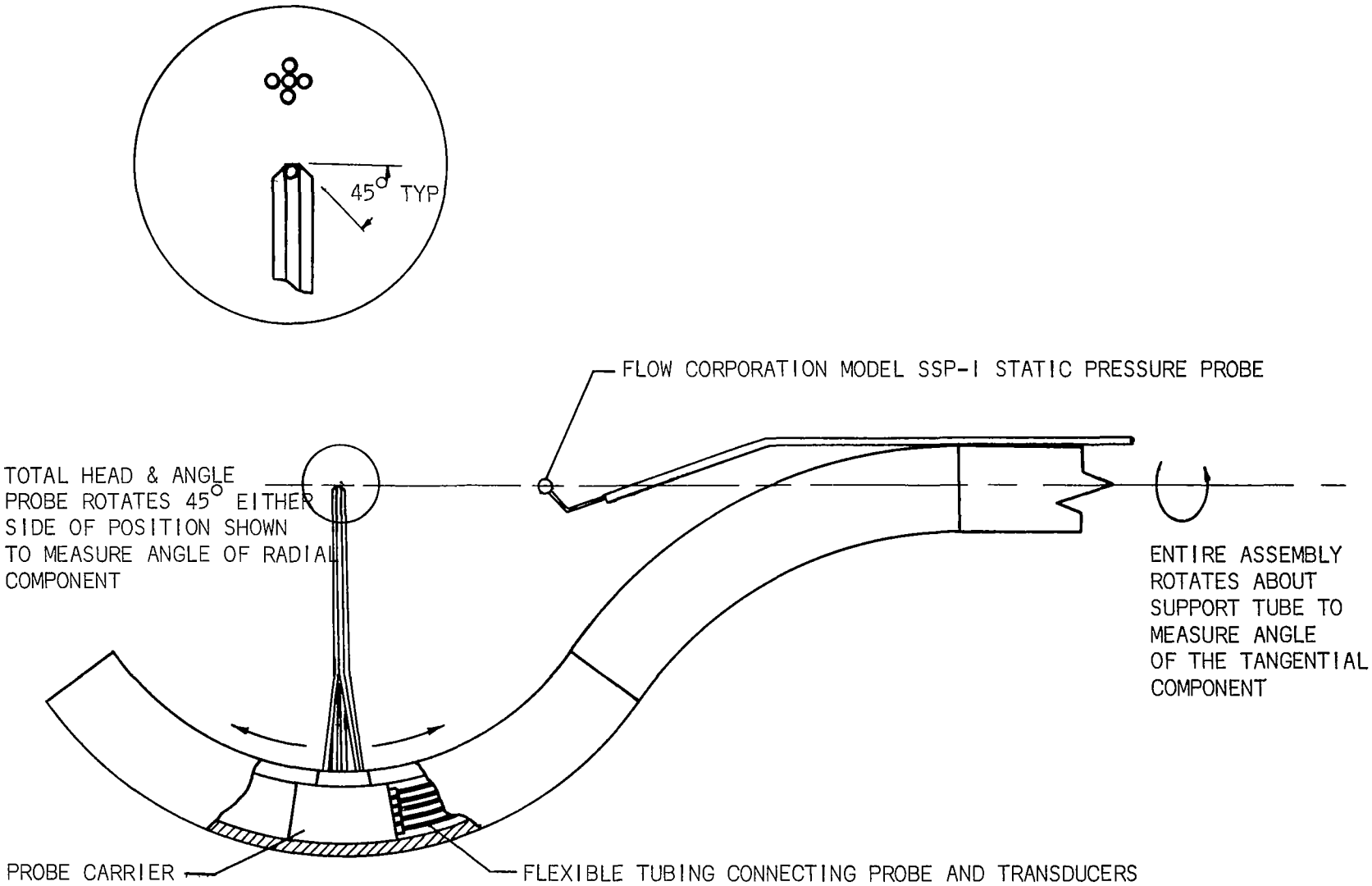

Figure 3 Probe Assembly

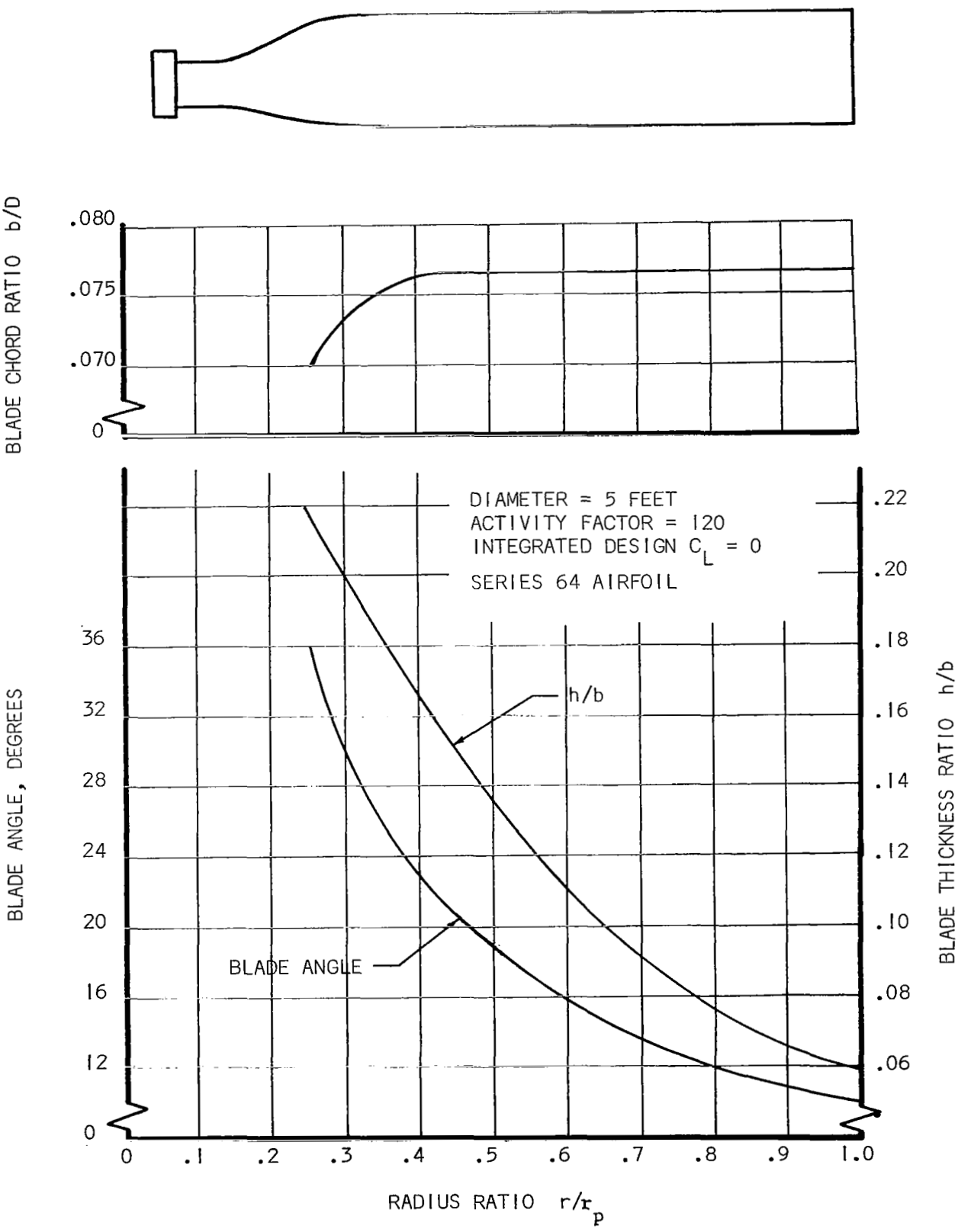

Figure 4 Propeller A

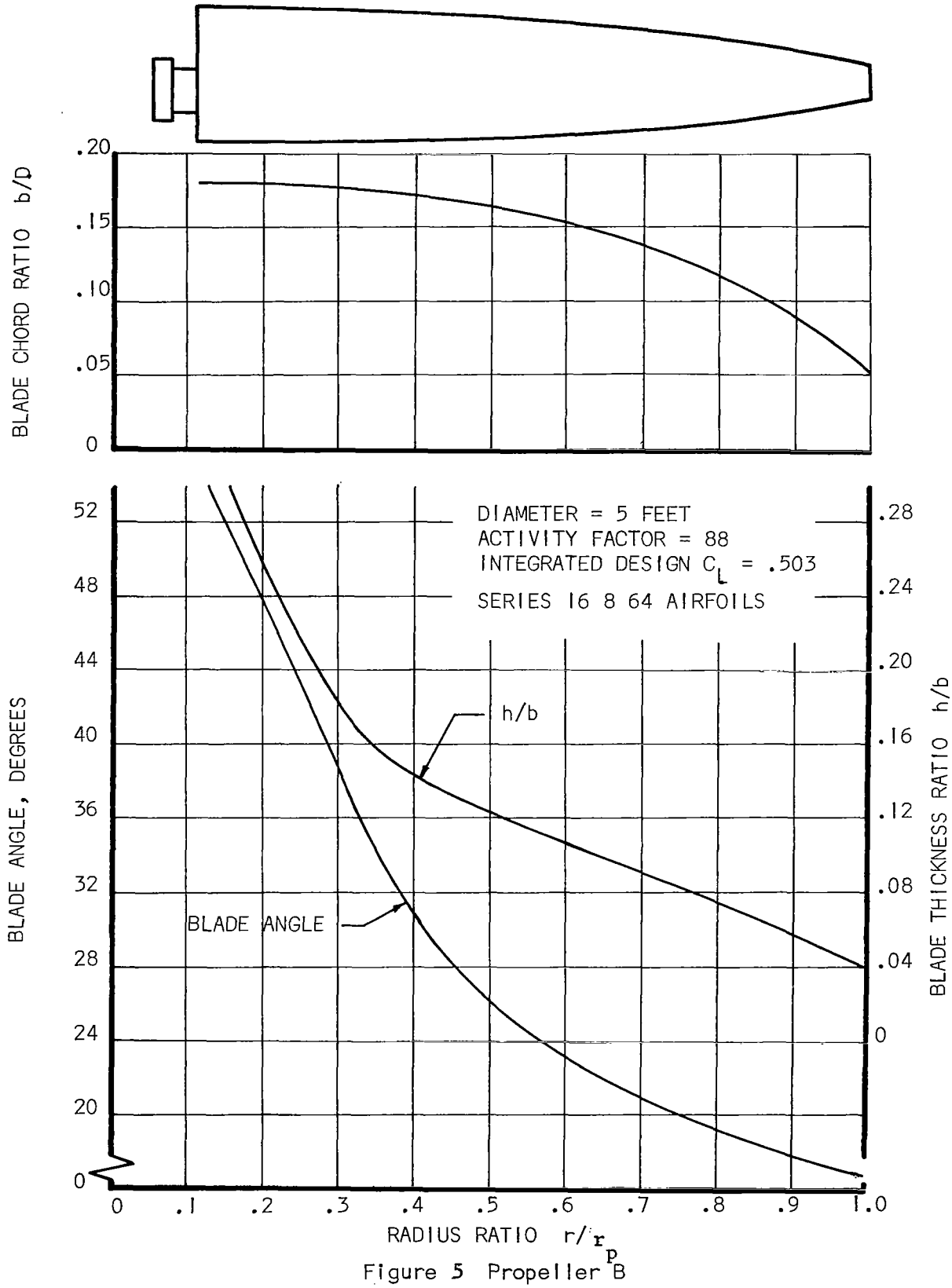

Figure 5 Propeller B

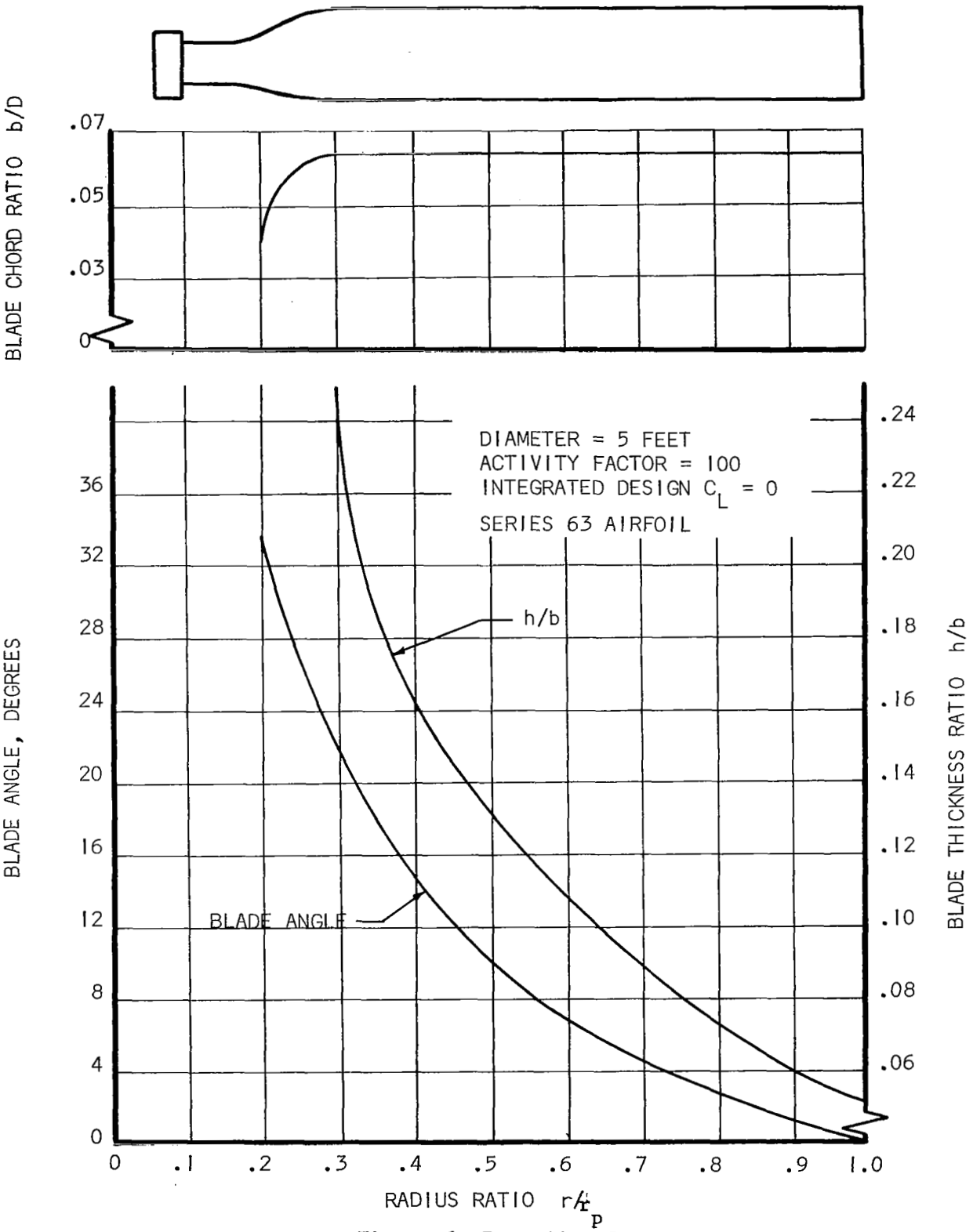

Figure 6 Propeller C

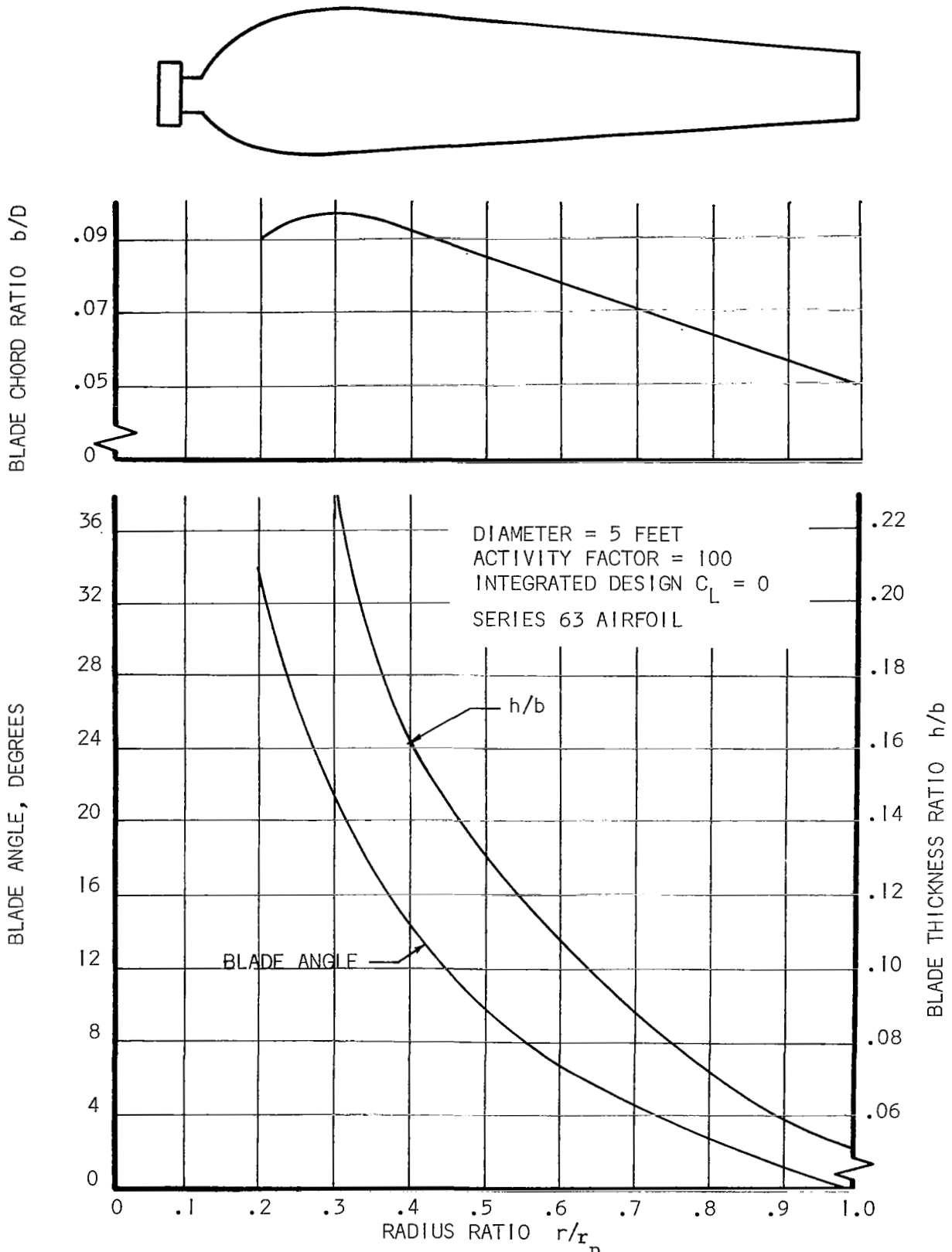

Figure 7 Propeller D

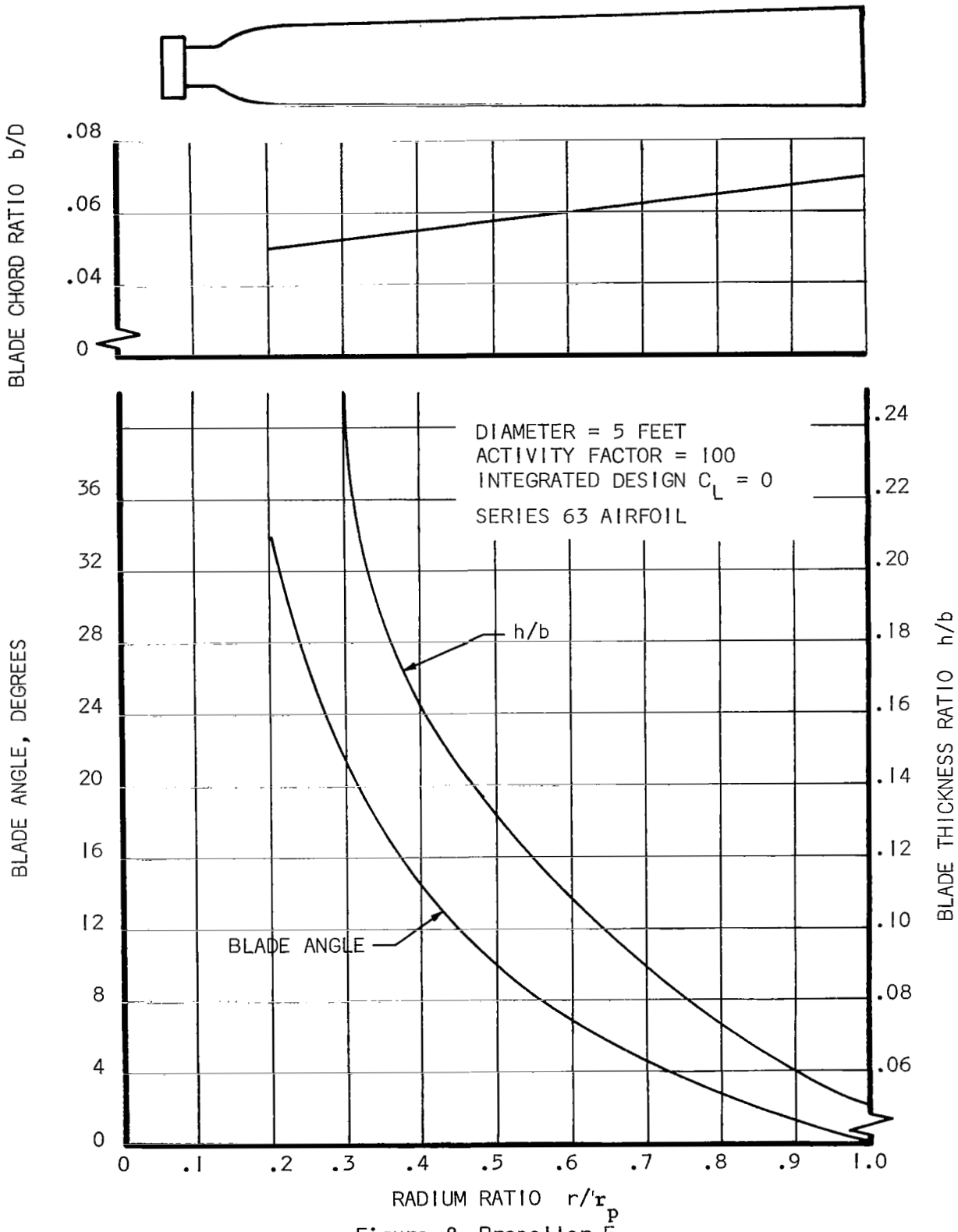

Figure 8 Propeller E

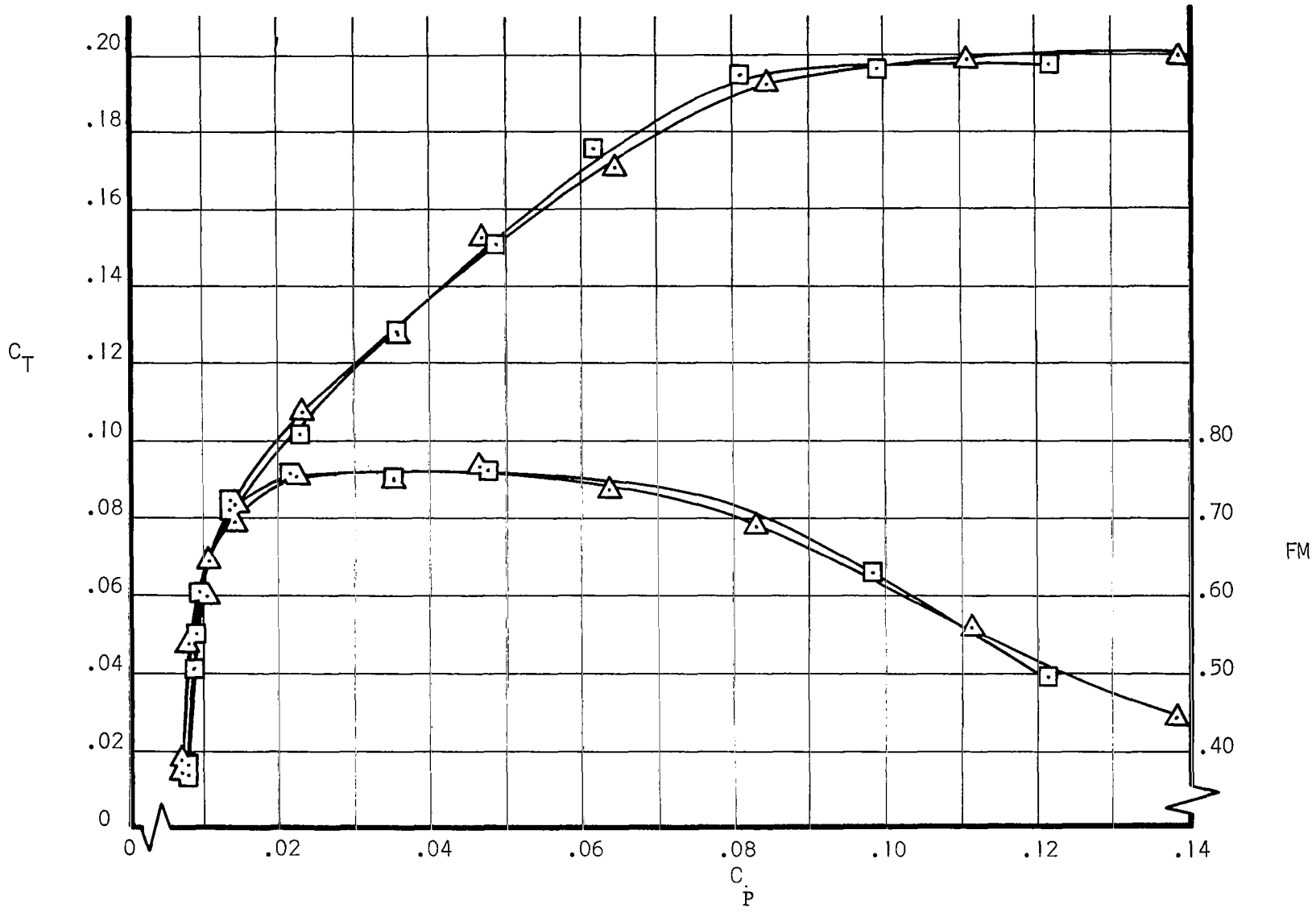

Figure 9 C_T Versus C_P For Propeller B

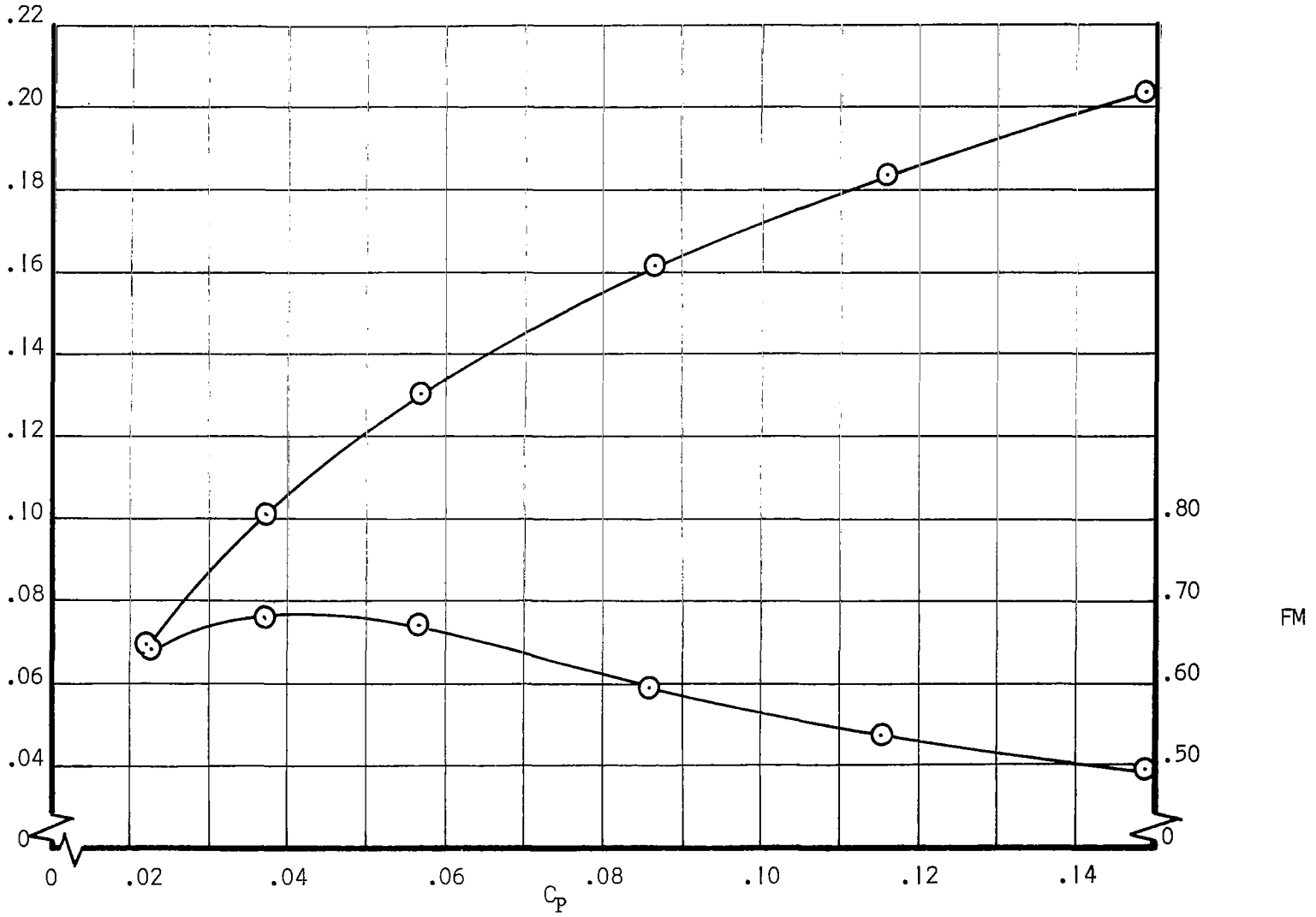

Figure 10 C_T Versus C_P for Propeller A

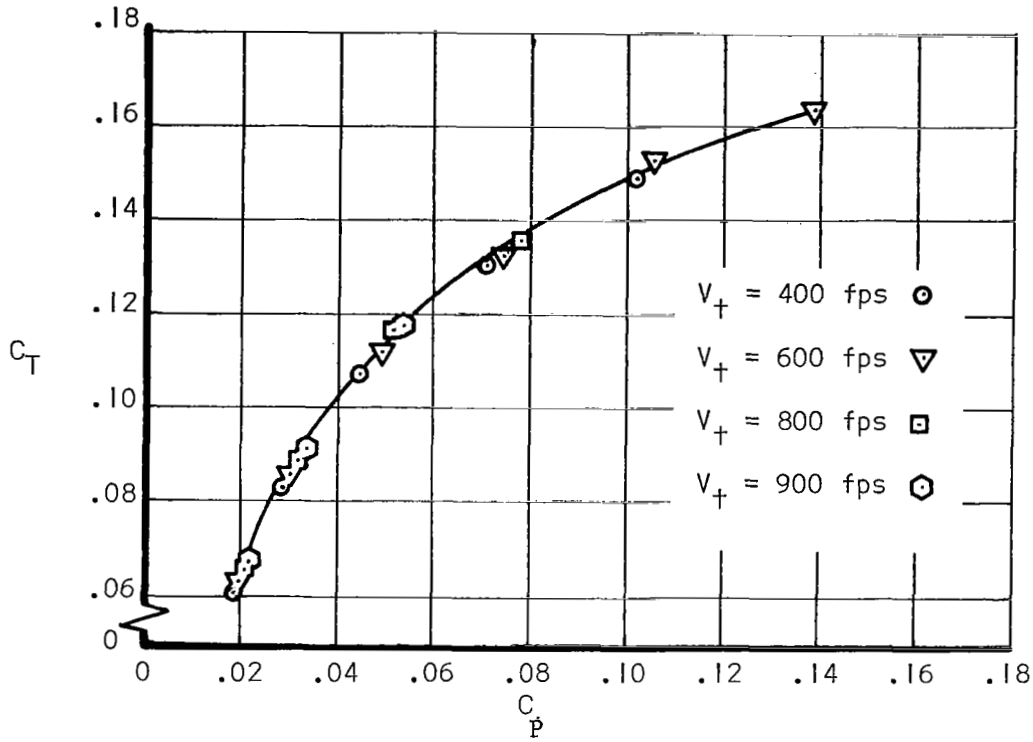

Figure 11 C_T Versus C_P For Propeller C

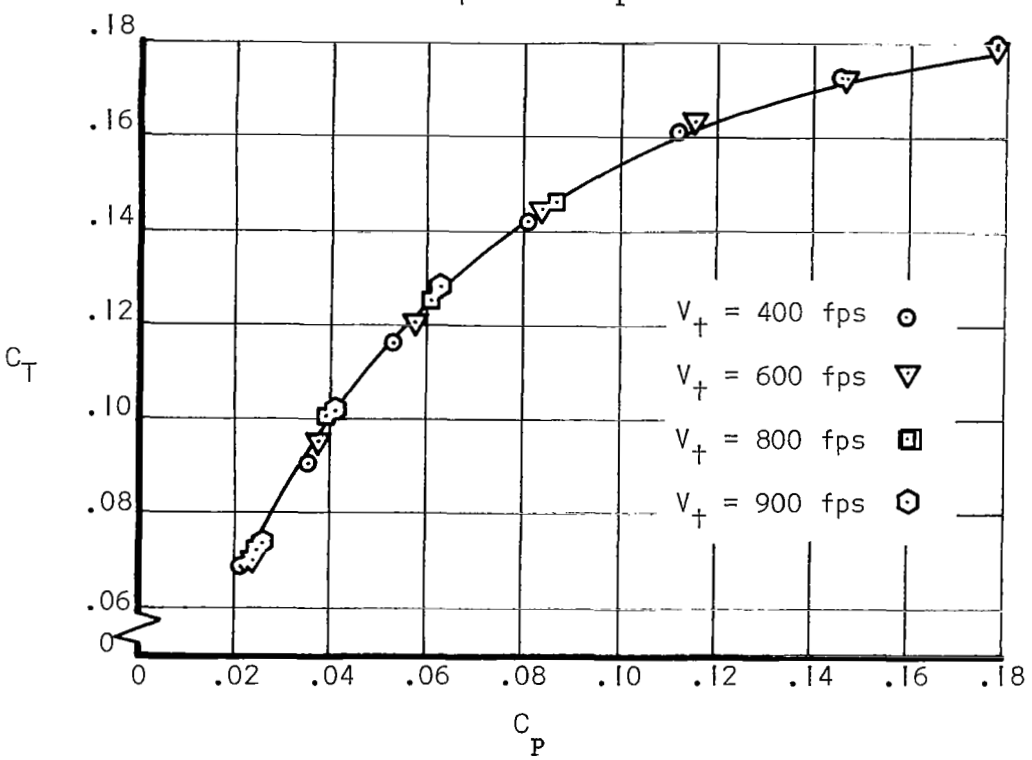

Figure 12 C_T Versus C_P For Propeller D

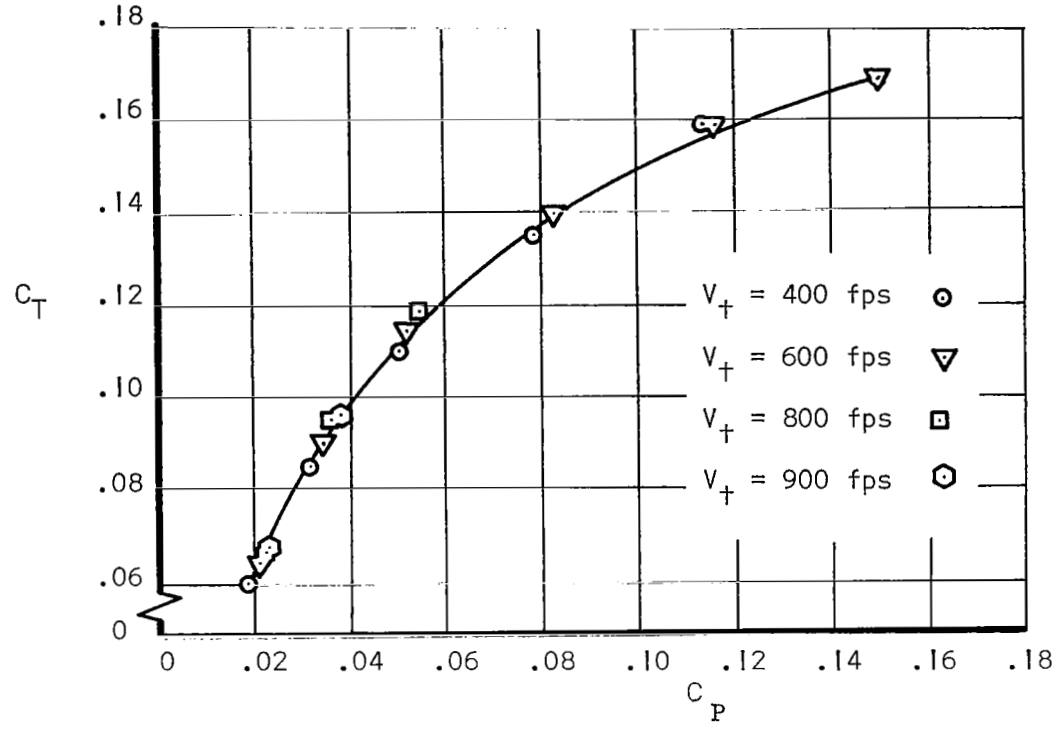

Figure 13 C_T Versus C_P for Propeller E

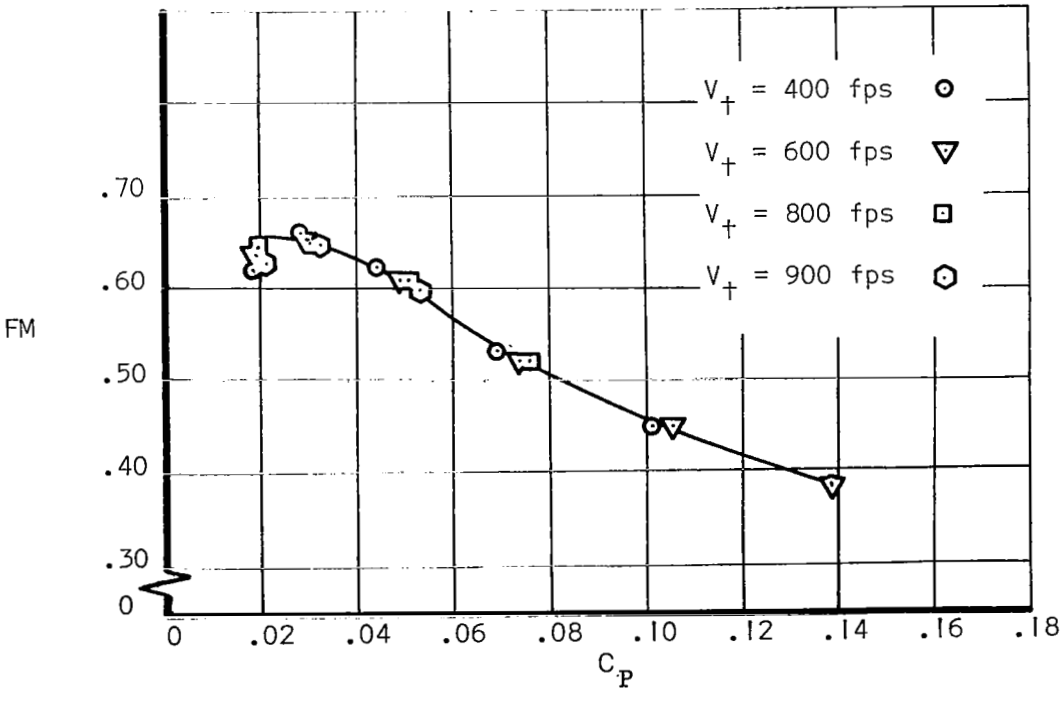

Figure 14 FM Versus C_P for Propeller C

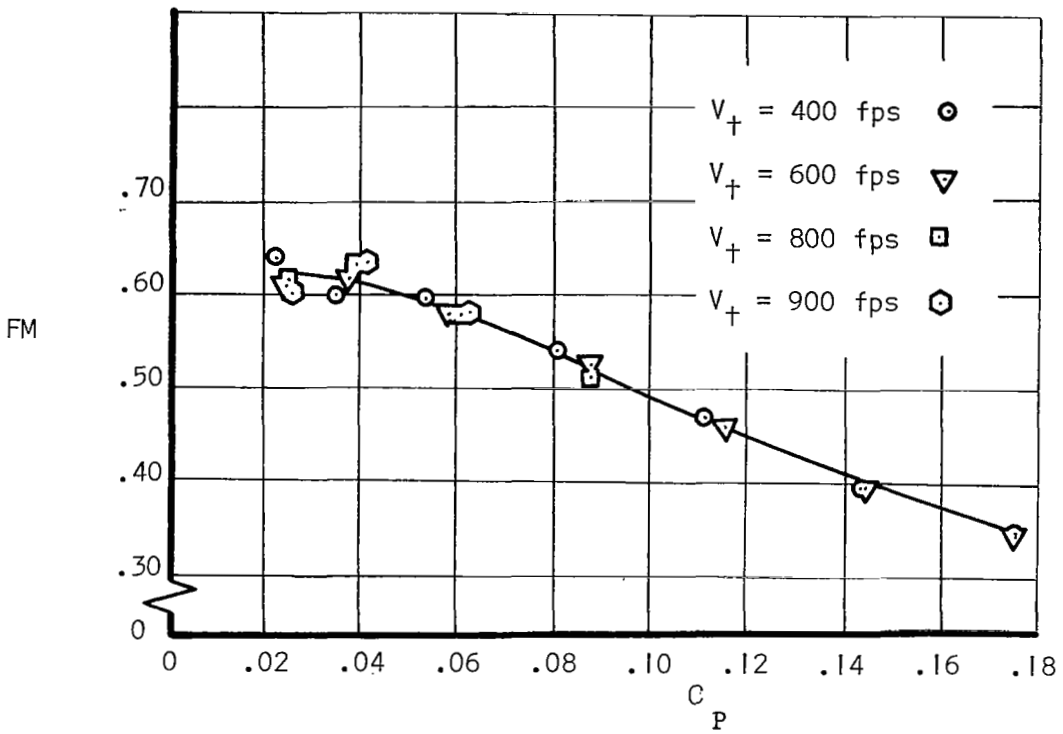

Figure 15 FM versus C_P for Propeller D

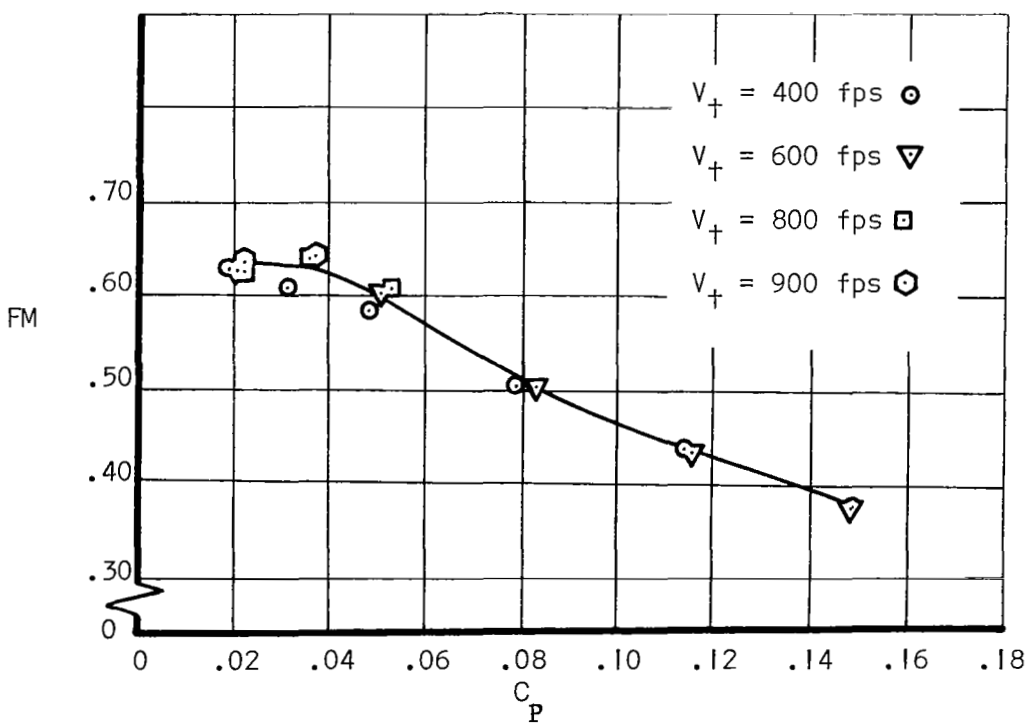

Figure 16 FM versus C_P for Propeller E

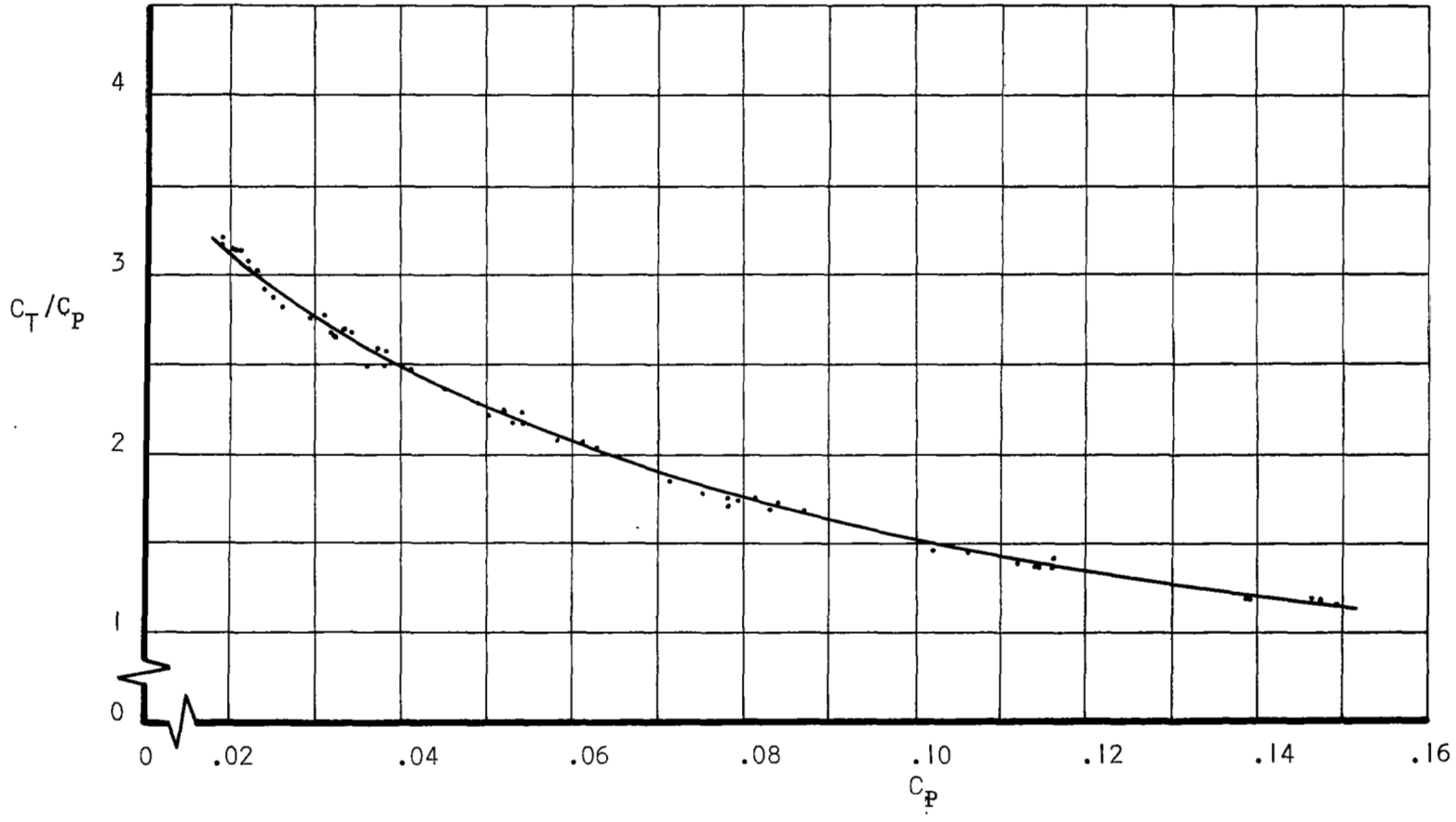

Figure 17 C_T/C_P Versus C_P For All Propellers

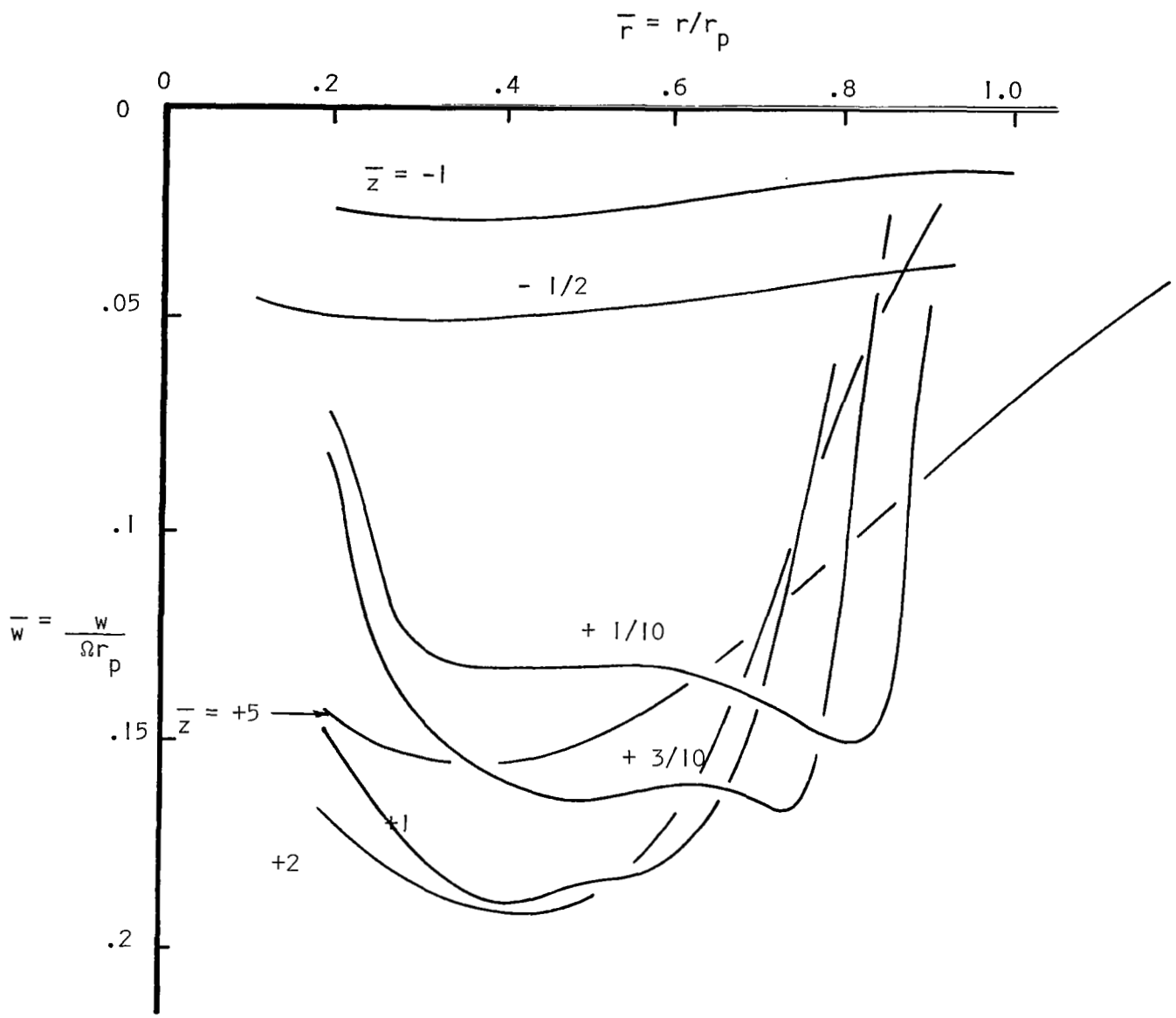

Figure 18 Axial Velocity Distribution

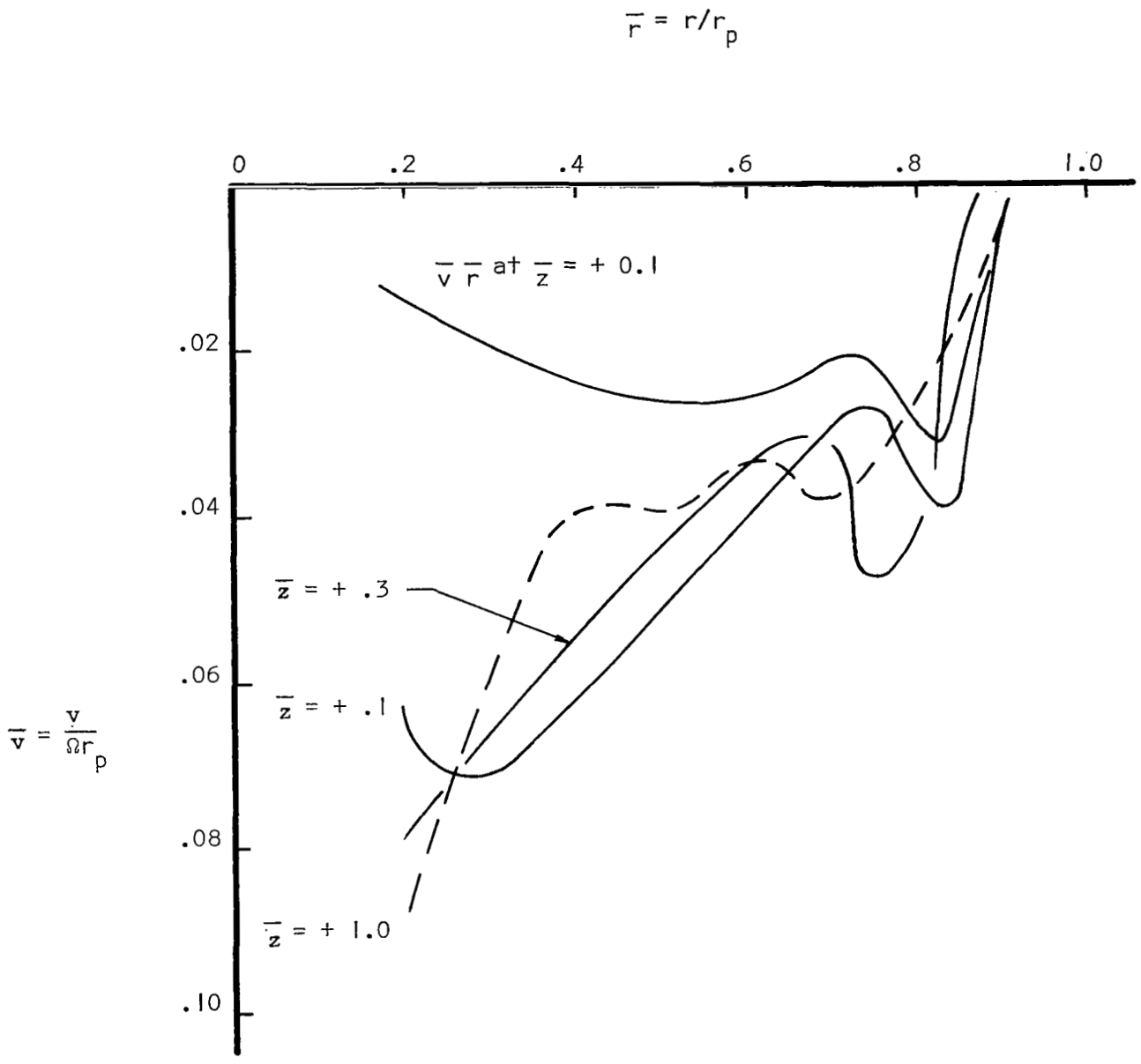

Figure 19 Tangential Velocity Distributions